Three Dimensionally Ordered Macroporous Layered Double Hydroxides: Preparation by Templated Impregnation/ Coprecipitation and Pattern Stability upon Calcination†

Erwan Géraud,‡ Salah Rafqah,‡,§ Mohamed Sarakha,§ Claude Forano,‡ Vanessa Prevot,*,‡ and Fabrice Leroux‡

Laboratoire des Matériaux Inorganiques, UMR CNRS 600, and Laboratoire de Photochimie Moléculaire et Macromoléculaire, UMR CNRS 6505, Université Blaise Pascal, 24, avenue des Landais, 63177 Aubière Cedex, France

Received September 26, 2007. Revised Manuscript Received November 9, 2007

Three dimensionally ordered macroporous layered double hydroxides (3-DOM LDH) have been synthesized using sacrificial polystyrene (PS) colloidal crystal templates impregnated by divalent and trivalent metal salts. LDH spatially confined coprecipitation occurs during soaking in NaOH solution, and the PS template is subsequently removed by dissolution to preserve the hydroxyl structure. This synthetic process can be applied to a wide range of LDH compositions (M^{II}: Mg, Ni, Co, Zn and M^{III}: Al, Cr). On the basis of XRD, SEM, TEM, chemical analysis, nitrogen adsorption, XAS experiments, and TGA, structural, textural, and thermal properties of these new nanostructured LDH particles are described. In particular, the study shows that both macro- and mesoporosity can be present and that the macroporosity is maintained after calcination at temperatures as high as 800 °C, giving rise to the presence of macroporous metal and mixed metal oxides. The photocatalytic activity experiments indicate that decatungstate intercalated into the 3-DOM LDH exhibits a higher photocatalytic activity for the photodegradation of 2,6-dimethylphenol than the decatungstate intercalated into the standard coprecipitated LDH parent material.

Introduction

Layered double hydroxides (LDHs), also called hydrotalcite-like compounds,[1–3] possess a layered structure of general formula $[M^{II}_{1-x}M^{III}_{x}(OH)_2]^{x+}[X^{q-}_{x/q}(H_2O)_n]^{x-}$ (hereafter noted as $M^{II}M^{III}-$). The positive charge generated by the substitution of a part of the divalent cations by trivalent cations in the brucite-like layers is compensated by the presence of anions in the interlayer space. Because of their lamellar features and high versatility of composition, LDHs are potentially interesting in various fields of application[4] such as anion exchangers, adsorbents,[5] catalysts, and precursors of catalysts.[6,7] Recently, a lot of attention has been devoted to their use in new fields of materials research such as inorganic fillers,[8] precursors of nanostructured oxides,[9] even as sensors[10] or biosensors,[11] and biomolecule carriers.[12] Classically, LDHs are prepared by coprecipitation methods[13,14] involving mixtures of divalent and trivalent metal salts at fixed pH in aqueous solution leading to particles with an inhomogeneous distribution in size and shape and an uncontrolled aggregation. Because the control of the textural properties in terms of morphology, particle size, specific area, and pore structure is of great interest[15] in most of the mentioned applications, much attention has been paid to develop original synthetic pathways, especially to obtain nanostructured LDH materials, which might display new textural properties. Indeed, new trends have been reported; for instance, Duan et al. optimized the preparation of LDH particles with the lateral size distributed in a narrow range using a colloid mill to separate the nucleation and the crystal

† Part of the "Templated Materials Special Issue".

* Corresponding author. E-mail: vanessa.prevot@univ-bpclermont.fr.
‡ Laboratoire des Matériaux Inorganiques.
§ Laboratoire de Photochimie Moléculaire et Macromoléculaire.

(1) Braterman, P. S.; Xu, Z. P.; Yarberry, F. Layered double hydroxides (LDHs). In *Handbook of Layered Materials*; Auerbach, S. M., Carrado, K. A., Dutta, P. K., Eds.; Marcel Dekker: New York, 2004; p 373.
(2) *Structure and bonding: Layered Double Hydroxides*; Duan, X., Evans, D. G., Eds.; Springer: Berlin/Heidelberg, 2006; Vol. 119.
(3) Rives, V. *Layered Doubles Hydroxides: Present and Future*; Nova Science Publisher: New York, U.S.A., 2001.
(4) Williams, G. R.; O'Hare, D. *J. Mater. Chem.* **2006**, *16*, 3065.
(5) Forano, C. Environmental remediation involving layered double hydroxides. In *Clays Surfaces: Fundamentals and applications*; Wypych, F., Satyanarayana, K. G., Eds.; Elsevier: New York, 2004; Vol. 1, p 425.
(6) Tichit, D.; Gerardin, C.; Durand, R.; Coq, B. *Top. Catal.* **2006**, *39*, 89.
(7) Vaccari, A. *Appl. Clay Sci.* **1999**, *14*, 161.
(8) Leroux, F.; Besse, J.-P. *Chem. Mater.* **2001**, *13*, 3507.
(9) Zou, L.; Li, F.; Xiang, X.; Evans, D. G.; Duan, X. *Chem. Mater.* **2006**, *18*, 5852.
(10) Darder, M.; Lopez-Blanco, M.; Aranda, P.; Leroux, F.; Ruiz-Hitzky, E. *Chem. Mater.* **2005**, *17*, 1969.
(11) Forano, C.; Vial, S.; Mousty, C. *Curr. Nanosci.* **2006**, *2*, 283.
(12) Choy, J.-H.; Choi, S.-J.; Oh, J.-M.; Park, T. *Appl. Clay Sci.* **2007**, *36*, 122.
(13) de Roy, A.; Forano, C.; Besse, J. P. Layered double hydroxides: Synthesis and post-synthesis modifications. In *Layered Double Hydroxides*; Rives, V., Ed.; Nova Science Publisher: New York, 2001; p 1.
(14) He, J.; Wei, M.; Li, B.; Kang, Y.; Evans, D. G.; Duan, X. *Struct. Bonding (Berlin)* **2006**, *119*, 89.
(15) Abello, S.; Medina, F.; Tichit, D.; Perez-Ramirez, J.; Cesteros, Y.; Salagre, P.; Sueiras, J. E. *Chem. Commun.* **2005**, 1453.

10.1021/cm702755h CCC: $40.75
Published on Web 12/21/2007

growth.[16,17] In parallel, nanometer sized ZnAl−LDH particles have been prepared under steady state conditions of coprecipitation.[18] In other approaches, some authors investigated the possibility to obtain nanosheets[19–28] which might be further used[29] either as initial building blocks to design and fabricate nanostructured films[30–32] and/or materials or as colloidal fillers within polymer nanocomposites.[8,33] These successful attempts to delaminate the LDH lamellar assembly in different solvents were reported using or not using organic anions as modifiers. Aside from this and much closer to our present work, LDH synthesis may be carried out in a confined medium such as in a reverse microemulsion as reported brilliantly by O'Hare et al.[34,35]

Another elegant template method to produce hollow nanoshells of LDH was reported by Sasaki et al. in which exfoliated LDH nanosheets were deposited layer by layer onto the surface of polystyrene (PS) beads, used here as a sacrificial template.[36] Even if such sacrificial template methods are known to offer an efficient method for the fabrication of nanostructured materials in other inorganic systems, only few attemps were reported so far. We succeeded recently in synthesizing three dimensionally ordered macroporous (3-DOM) MgAl−LDHs (hydrotalcite) by using a colloidal crystal templating method.[37] The procedure consists of infiltrating the interstitial voids of the colloidal crystal template with the precursor solution yielding macroporous inorganic structures with interconnected macropores after the fluid−solid transformation[7] and subsequent removal of the colloidal spheres array by calcination or dissolution. Such self-assembled colloidal crystals, also called synthetic opals, were largely used to template materials,[38–40] and a large number of porous materials may be readily obtained, especially those presenting continuous networks or aggregation of three-dimensional (3D) particles such as silica,[41–43] metals,[44–47] semiconductors,[48] metal oxides,[43,47,49–52] mixed metal oxides,[53] carbon,[54,55] and polymers.[56–58] So far, only few results have been reported on the nanostructuration of anisotropic systems[54,59] such as platelet-shaped particles. However, as an alternative to the traditional hydrolysis of metal alkoxide, Stein et al. reported the preparation of 3-DOM metal oxides and carbonate using the templated precipitation of transition metal salts by reacting with oxalic acids into the voids of the colloidal crystal.[60] Inspired by this, we investigated the possibility to merge the traditional LDH coprecipitation method with the PS colloidal crystal templating method[37] to prepare 3-DOM hydrotalcite from successive impregnation cycles allowing hydroxide precipitation around the beads. The paper investigates the extension of this templating method to the synthesis of various 3-DOM LDH type materials known not only for their thermal instability but also for their potential relevance in catalytic applications, such as those using cations as Ni, Co, Zn, and Cr, as well as the possibility of substituting cations to form mixed compositions such as MgNiAl−, MgCoAl−, and MgFeAl−. To obtain a macroporous open LDH framework, the PS array should systematically be removed. Owing to the LDH thermal instability, dissolution rather than calcination of the PS beads was preferred. The structural, textural, and thermal features of the as-prepared LDHs were detailed on the basis of chemical analysis, data

(16) Li, F.; Jiang, X.; Evans, D. G.; Duan, X. *J. Porous Mater.* **2005**, *12*, 55.
(17) Zhao, Y.; Li, F.; Zhang, R.; Evans, D. G.; Duan, X. *Chem. Mater.* **2002**, *14*, 4286.
(18) Chang, Z.; Evans, D. G.; Duan, X.; Vial, C.; Ghanbaja, J.; Prevot, V.; de Roy, M.; Forano, C. *J. Solid State Chem.* **2005**, *178*, 2766.
(19) Adachi-Pagano, M.; Forano, C.; Besse, J.-P. *Chem. Commun.* **2000**, 91.
(20) Hibino, T. *Chem. Mater.* **2004**, *16*, 5482.
(21) Hibino, T. *Encycl. Nanosci. Nanotechnol.* **2004**, *7*, 657.
(22) Hibino, T.; Kobayashi, M. *J. Mater. Chem.* **2005**, *15*, 653.
(23) Jaubertie, C.; Holgado, M. J.; San Roman, M. S.; Rives, V. *Chem. Mater.* **2006**, *18*, 3114.
(24) Leroux, F.; Adachi-Pagano, M.; Intissar, M.; Chauviere, S.; Forano, C.; Besse, J.-P. *J. Mater. Chem.* **2001**, *11*, 105.
(25) Li, L.; Ma, R.; Ebina, Y.; Iyi, N.; Sasaki, T. *Chem. Mater.* **2005**, *17*, 4386.
(26) Liu, Z.; Ma, R.; Osada, M.; Iyi, N.; Ebina, Y.; Takada, K.; Sasaki, T. *J. Am. Chem. Soc.* **2006**, *128*, 4872.
(27) Venugopal, B. R.; Shivakumara, C.; Rajamathi, M. *J. Colloid Interface Sci.* **2006**, *294*, 234.
(28) Wu, Q.; Olafsen, A.; Vistad, O. B.; Roots, J.; Norby, P. *J. Mater. Chem.* **2005**, *15*, 4695.
(29) Narita, E.; Hirahara, H.; Aizawa, S.; Saito, H. Method for delamination of layered double hydroxides, dispersions containing delaminated layered double hydroxides, thin films of layered double hydroxides, and their manufacture. Jpn. Patent 2002-359615, 2004 (Jpn. Pat. Appl. 189671).
(30) Okamoto, K.; Sasaki, T.; Fujita, T.; Iyi, N. *J. Mater. Chem.* **2006**, *16*, 1608.
(31) Gardner, E.; Huntoon, K. M.; Pinnavaia, T. J. *Adv. Mater.* **2001**, *13*, 1263.
(32) Itaya, K.; Chang, H.-C.; Uchida, I. *Inorg. Chem.* **1987**, *26*, 624.
(33) O'Leary, S.; O'Hare, D.; Seeley, G. *Chem. Commun.* **2002**, 1506.
(34) Hu, G.; O'Hare, D. *J. Am. Chem. Soc.* **2005**, *127*, 17808.
(35) Hu, G.; Wang, N.; O'Hare, D.; Davis, J. *Chem. Commun.* **2006**, 287.
(36) Li, L.; Ma, R.; Iyi, N.; Ebina, Y.; Takada, K.; Sasaki, T. *Chem. Commun.* **2006**, 3125.
(37) Geraud, E.; Prevot, V.; Ghanbaja, J.; Leroux, F. *Chem. Mater.* **2006**, *18*, 238.
(38) Schroden, R. C.; Stein, A. 3D ordered macroporous materials. In *Colloids and Colloid Assemblies*; Caruso, F., Ed.; Wiley-VCH: New York, 2004; p 465.
(39) Stein, A. *Microporous Mesoporous Mater.* **2001**, *44–45*, 227.
(40) Stein, A.; Schroden, R. C. *Curr. Opin. Solid State Mater. Sci.* **2001**, *5*, 553.
(41) Velev, O. D.; Jede, T. A.; Lobo, R. F.; Lenhoff, A. M. *Nature* **1997**, *389*, 447.
(42) Velev, O. D.; Jede, T. A.; Lobo, R. F.; Lenhoff, A. M. *Chem. Mater.* **1998**, *10*, 3597.
(43) Holland, B. T.; Blanford, C. F.; Do, T.; Stein, A. *Chem. Mater.* **1999**, *11*, 795.
(44) Feng, M.; Puddephatt, R. J. *Chem. Mater.* **2003**, *15*, 2696.
(45) Jiang, P.; Cizeron, J.; Bertone, J. F.; Colvin, V. L. *J. Am. Chem. Soc.* **1999**, *121*, 7957.
(46) Wijnhoven, J. E. G. J.; Zevenhuizen, S. J. M.; Hendriks, M. A.; Vanmaekelbergh, D.; Kelly, J. J.; Vos, W. L. *Adv. Mater.* **2000**, *12*, 888.
(47) Yan, H.; Blanford, C. F.; Holland, B. T.; Parent, M.; Smyrl, W. H.; Stein, A. *Adv. Mater.* **1999**, *11*, 1003.
(48) Braun, P. V.; Wiltzius, P. *Adv. Mater.* **2001**, *13*, 482.
(49) Chi, E. O.; Kim, Y. N.; Hur, N. H. *Chem. Mater.* **2003**, *15*, 1929.
(50) Hant, S. M.; Attard, G. S.; Riddle, R.; Ryan, K. M. *Chem. Mater.* **2005**, *17*, 1434.
(51) Holland, B. T.; Blanford, C.; Stein, A. *Science* **1998**, *281*, 538.
(52) Wijnhoven, J. E. G. J.; Vos, W. L. *Science* **1998**, *281*, 802.
(53) Sadakane, M.; Asanuma, T.; Kubo, J.; Ueda, W. *Chem. Mater.* **2005**, *17*, 3546.
(54) Lei, Z.; Zhang, Y.; Wang, H.; Ke, Y.; Li, F.; Li, J.; Xing, J. *J. Mater. Chem.* **2001**, *11*, 1975.
(55) Zakhidov, A. A.; Baughman, R. H.; Iqbak, Z.; Cui, C. X.; Khayrullin, I.; Dantas, S. O.; Marti, J.; Ralchenko, V. G. *Science* **1998**, *282*, 897.
(56) Gates, B.; Yin, Y.; Xia, Y. *Chem. Mater.* **1999**, *11*, 2827.
(57) Jiang, P.; Hwang, K. S.; Mittleman, D. M.; Bertone, J. F.; Colvin, V. L. *J. Am. Chem. Soc.* **1999**, *121*, 11630.
(58) Park, S. H.; Xia, Y. *Adv. Mater.* **1998**, *10*, 1045.
(59) Ergang, N. S.; Lytle, J. C.; Yan, H.; Stein, A. *J. Electrochem. Soc.* **2005**, *152*, A1989.
(60) Yan, H.; Blanford, C. F.; Holland, B. T.; Smyrl, W. H.; Stein, A. *Chem. Mater.* **2000**, *12*, 1134.

powder X-ray diffraction (XRD) experiments, scanning electron microscopy (SEM), transmission electron microscopy (TEM) images, X-ray absorption spectroscopy (XAS) measurements, and thermogravimetric analysis (TGA). Finally to validate our assumptions, the photocatalytic activity of decatungstate intercalated 3-DOM MgAl− was evaluated by the photodegradation of 2,6-dimethylphenol (DMP).

Experimental Section

Materials. Monomer styrene was distilled just before use to remove any traces of the inhibitor. Monodisperse PS beads ranging from 150 to 1000 nm were synthesized by the "emulsifier-free" emulsion polymerization of styrene as described elsewhere.[61] In this study, PS spheres of 820 nm are used and disposed in closed-packed colloidal arrays by centrifugation of the bead suspensions (2 wt %) at 1200 rpm for 14 h. After removal of water, the resulting solid was air-dried. Deionized and decarbonated water was used throughout the experiments. All other chemicals were reagent grade and used as received.

Synthesis of Ordered Macroporous LDHs. Metal chlorides water/ethanol mixture (50:50) solutions (1 M) were prepared in appropriate metal cation amounts with respect to a ratio M^{II}/M^{III} of 2. When three different metal cations were implied, that is, for MgNiAl−, MgCoAl−, and MgFeAl−, the global ratio M^{II}/M^{III} was kept at 2, with Mg/(Ni or Co) = 1 and Fe/Al = 1. Millimeter-scale pieces of closed-packed arrays of the PS spheres (∼1 g) were deposited into an Erlenmeyer flask to serve as template, and 6 mL of the precursor solution was added to infiltrate the PS colloidal crystals. After 24 h, the excess solution was removed by a slight filtration through a Buchner funnel. The obtained samples were allowed to dry in air at room temperature overnight. Then, the dried metallic salt impregnated crystals (∼1 g) were soaked in 6 mL of sodium hydroxide aqueous solution (2 M) for 24 h to achieve coprecipitation. For the ZnCr−LDH composition, special care was taken to stabilize the pH at 5, while for the other compositions that were tried much higher values of the pH ($8 < pH < 11$) were suitable. After removal of the excess basic solution, the samples were washed with water and dried, and the PS templates were subsequently removed by dissolution utilizing three successive toluene or tetrahydrofuran (THF)−acetone (1:1) soakings (1 g/10 mL). A few hundred micrometer sized aggregates of particles were obtained after the dissolution step.

Intercalation of the Decatungstate Anion. 3-DOM MgAl−dodecyl sulfate (DDS) ion-exchange precursor was prepared as previously reported:[62] A 50 mg quantity of 3-DOM MgAl was heated at 400 °C and immediately immersed into 50 mL of 0.1 M DDS aqueous solution for 1 day under a nitrogen atmosphere, washed with water, and dried.

To preserve the stability of the LDH structure, the anion exchange with the decatungstate anion was carried out in a basic medium. The synthesis of the decatungstate intercalated MgAl LDH was undertaken as follows: A solution of the decatungstate anion, $W_{10}O_{32}^{4-}$, was prepared beforehand under backward flow in absolute ethanol. The LDH precursor was added in suspension to the previous ethanol solution under a nitrogen flow. This mixture was conditioned, under agitation, at 65 °C using an oil bath for 2 days and then centrifugated. The obtained suspension was carefully washed with distilled water and dried overnight at 100 °C.

For comparison purposes, the Mg_2Al−Cl precursor was prepared by coprecipitation following the method previously described.[62] DDS was intercalated by a standard anionic exchange in using an amount of DDS twice larger than the anion exchange capacity of Mg_2Al−Cl, hereafter denoted MgAl−DDS_{stand}. Decatungstate was intercalated into MgAl−DDS_{stand} by following a procedure similar to that described for the macroporous compounds (hereafter denoted MgAl−$W_{10}O_{32stand}$).

Characterization. The PS bead sizes were measured from dilute suspensions with a Malvern Zetasizer (Nano ZS). Chemical analyses (Mg, Ni, Co, Zn, Al, Cr, Fe, C, H) were performed by inductively coupled plasma atom emission spectroscopy at the Vernaison Analysis Center of CNRS (France). Powder XRD experiments were carried out with a Siemens D501 X-ray diffractometer using Cu Kα radiation ($\lambda = 1.5415$ Å) and fitted with a graphite back-end monochromator. Diagrams were acquired from 5° to 70° in 2θ using a step of 0.02° and a counting time per step of 10 s. In situ XRD patterns were obtained by a X'Pert Pro Philips diffractometer with a diffracted beam graphite monochromator using a Cu Kα ($\lambda = 1.54$ Å) radiation source equipped with a high-temperature chamber (Anton Paar HTK-16). Diffractograms were recorded in the 2θ range of 2–70° with a step of 0.013° and a counting time per step of 20 s. SEM characteristics of the samples were imaged by either a JEOL 5190 microscope operated at 15 keV or a Zeiss supra 55 FEG-VP operating at 3 keV. Specimens were mounted on conductive carbon adhesive tabs and imaged after carbon sputter coating to make them conductive. TEM images were taken using a Hitachi 7650 microscope at an acceleration voltage of 80 kV. Samples were dispersed in ethanol, and then one droplet of the suspension was applied to a 400 mesh holey carbon-coated copper grid and left to dry in air. The N_2 adsorption isotherms at the liquid nitrogen temperature were recorded on a Fison SP1920 instrument. Prior to the experiments, the compounds were submitted to a pretreatement (80 °C, 12 h under vacuum) to remove the adsorbed water. Attenuated total reflectance Fourier transform infrared (FTIR) spectra were measured in the range of 400–4000 cm^{-1} on an FTIR Nicolet 5700 spectrometer (Thermo Electron Corp.) equipped with a Smart Orbit accessory. X-ray absorption fine structure (EXAFS) studies were performed at Elletra (Trieste, Italy) using X-ray synchrotron radiation. Data were collected at room temperature in the transmission mode at the corresponding K edge (Co, 7708.9 eV; Ni, 8332.8 eV; Zn, 9658.6 eV). The absorbance, μ, was measured using a standard ion chamber before (I_0) and after (I) the sample was added, $\mu = \ln(I/I_0)$. The quantity of powdered samples was chosen to obtain edge jumps of about $\Delta\mu \approx 1$. A double-crystal Si (111) monochromator scanned the energy in 2 eV steps from 100 eV below to 900 eV above the Zn K absorption edge; three spectra were recorded for each sample. The accumulation time was 2 s per point. The pre- and post-edge backgrounds were obtained by fitting polynomials of order 1 and 5, respectively, and the absorbance was normalized using the Lengeler−Eisenberger method. Fourier transforms of the EXAFS spectra were made, after multiplication of the signal by a k^3 factor, over a 2.8–14 $Å^{-1}$ Kaiser apodization window with $\tau = 2.5$. The EXAFS spectra were analyzed using the classical plane-wave single scattering equation, $\chi(k) = S_0^2 \sum A_i(k) \sin[2kr_i + \varphi_i(k)]$, with the $A_i(k)$ amplitude equal to $(N_i/kr_i^2)F(k) \exp(-2k^2\sigma_i^2) \exp(-2r_i/\Gamma)$, where r_i is the interatomic distance for the ith shell of neighboring atoms around the central atom, φ_i is the total phase shift of the ith shell, N_i is the effective coordination number, σ_i is the Debye–Waller factor, Γ is the free mean path, and $F_i(k)$ is the backscattering amplitude. The residual ρ factor is defined as $\rho = [\sum(k^3\chi \exp(k) - k^3\chi \text{ theo}(k))^2/\sum(k^3\chi \exp(k))^2]^{1/2}$. Multiple scattering was not considered because it was expected to be insignificant for the nearest neighbor, P1 and P2

(61) Furusawa, K.; Norde, W.; Lyklema, J. *Kolloid Z. Z. Polym.* **1972**, *250*, 908.
(62) Geraud, E.; Prevot, V.; Leroux, F. *J. Phys. Chem. Solids* **2006**, *67*, 903.

(see text) and as the long metal to metal distance correlations P3 and P4 (see text) arising from multiple scattering phenomena were not refined. The contribution of the first two shells, P1 and P2, was extracted by a back Fourier transform in R space ($\Delta R \approx 2.4$ Å, $\Delta k \approx 10$ Å^{-1}) and then fitted by using theoretical functions as reported in the McKale et al.'s tables.[63] The program Round Midnight[64] (its use is found in refs 24, 65, and 66) was used to fit the $\chi(k)$ equation to the experimental signal by a least-squares fitting procedure. The fits for reference materials were carried out taking the data available in the literature. Zn_2Cr−LDH-CO_3^{2-}, MAl−LDH-Cl (M = Co, Ni) were taken as reference compounds, and the validity of the refinements were reported in previous contributions.[24,67,68] For the samples prepared by the sacrificial template and to estimate the relative part of the cations contributing to the metal−metal correlation, the number of backscattering atoms was free to move during the refinement. This guarantees all possible cation ratios for the second shell. The commonly accepted fitting accuracy is about 0.02 Å for the distance and 15−20% for the number of neighbors. Analyses using TGA were recorded on a Setaram TG-DTA 92 thermogravimetric analyzer in the temperature range of 25–1000 °C, with a heating rate of 5 °C/min.

Measurement of Photocatalytic Activity. The photocatalytic efficiency of $W_{10}O_{32}^{4-}$ intercalated MgAl LDH was studied using DMP as a model compound. The usual concentration of the photocatalyst was 1 g L^{-1}. The irradiation setup consisted of an elliptical stainless steel container that was used for both kinetic and analytical experiments. A high-pressure mercury lamp (Philips HPW type 125 W), whose main emission at 365 nm (93%) was selected by an inner filter, was located at a focal axis of the elliptical cylinder. The reactor, a water-jacketed Pyrex tube (diameter = 1.8 cm) was centered at the other focal axis. The solution was continuously stirred using a magnetic stirrer or an air flow. The disappearance of DMP and the formation of the byproduct were followed by high performance liquid chromatography (HPLC) using a Waters 540 HPLC chromatograph system equipped with a Waters 996 photodiode array detector. The experiments were performed by UV detection at 270 nm and by using a reverse phase Nucleodur column (C_{18}-5 μm; 250–4.6 mm). The flow rate was 1.0 mL min^{-1} with an injected volume of 50 μL. The elution was accomplished with acidified water and methanol (40:60 by volume).

Results and Discussion

Preparation and Characterization of the 3-DOM LDH. The successive steps of the impregnation−dissolution for the fabrication of the DOM LDH are illustrated in Figure 1. The PS colloidal crystal obtained by slow centrifugation displays a face-centered cubic packing. Upon soaking in a mixed metal salts solution, the voids between the spheres were filled, and upon drying, the mixed metal salts are maintained in the 3D array. To favor the infiltration, a water−ethanol mixture should be used to increase the diffusion within the voids and, therefore, the PS array wetting. The *in-situ* LDH coprecipitation is carried out by

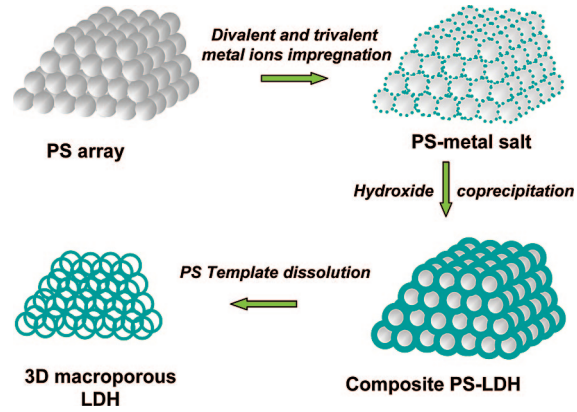

Figure 1. Schematic illustration of the successive steps for fabricating ordered macroporous LDH by a PS colloidal crystal template.

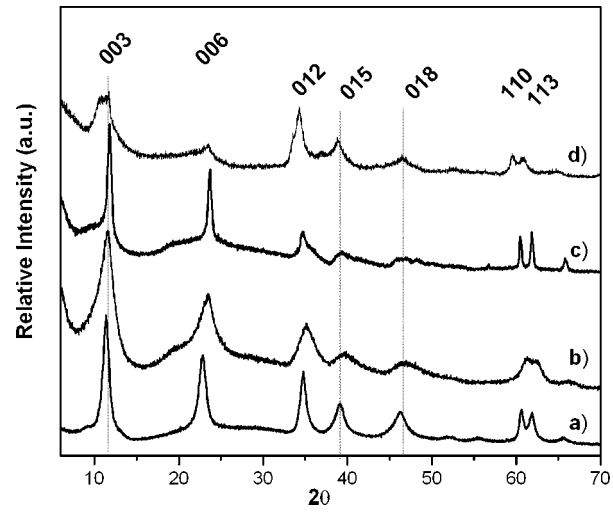

Figure 2. XRD patterns of (a) MgAl−, (b) NiAl−, (c) CoAl−, and (d) ZnCr− LDH matrixes obtained after templated synthesis.

further infiltration of the PS array by NaOH. Because the inorganic salts, such as NaCl and Na_2CO_3, also formed during the coprecipitation are water soluble, they are easily removed by washing. The PS template extraction by dissolution in a suitable solvent leads to a replica of the colloidal crystal but of reduced size.[38] At first, this synthetic procedure was applied to MgAl−, NiAl−, CoAl−, and ZnCr− compositions. XRD patterns recorded from the as-prepared samples (Figure 2) indicate that the desired LDH structure is systematically obtained as 00l basal lines series as well as asymmetric *hk*0 lines characteristic of ordering inside the LDH layer.[2,3] Nevertheless, the intensity and the width of the diffraction peaks show some differences depending on the compositions. Byproducts as hydroxides ($M^{II}(OH)_2$ or $M^{III}(OH)_3$) are not observed, indicating that homogeneous coprecipitation can be achieved using the confined templated synthesis by successive soakings. Assuming a 3R stacking, the lattice parameters are reported in Table 1. Note that the variation of the a parameter between the different LDH compositions is in agreement with the size of the divalent versus trivalent metal cations located in the sheet (following Vegard's law). Similar interlamellar distances are observed ($d \approx 0.76 \pm 0.01$ nm) corresponding to the intercalation of carbonate anions, confirmed by IR spectroscopy (see Supporting Information Figure S1). Because the syntheses were

(63) McKale, A. G.; Veal, B. W.; Paulikas, A. P.; Chan, S. K.; Knapp, G. S. *J. Am. Chem. Soc.* **1988**, *110*, 3763.
(64) Michalowicz, A. *J. Phys. IV* **1997**, *7*, 235.
(65) Intissar, M.; Jumas, J.-C.; Besse, J.-P.; Leroux, F. *Chem. Mater.* **2003**, *15*, 4625.
(66) Leroux, F.; Dewar, P.; Intissar, M.; Ouvrard, G.; Nazar, L. F. *J. Mater. Chem.* **2002**, 3245.
(67) Leroux, F.; El. Moujahid, M.; Taviot-Guého, C.; Besse, J.-P. *Solid State Sci.* **2001**, *3*, 81.
(68) Roussel, H.; Briois, V.; Elkaim, E.; de Roy, A.; Besse, J.-P. *J. Phys. Chem. B* **2000**, *104*, 5915.

Table 1. Chemical, Structural, and Porosity Data for 3-DOM LDH

matrix	chemical formula[a]	lattice parameter (nm)[b]		BET surface area (m^2/g)	macropore diameter (nm)[c]	wall thickness (nm)[c]	shrinkage %	total weight loss[d] %
		c	*a*					
MgAl−	$Mg_{1.9}Al(OH)_{5.8}(CO_3)_{0.51}$, nH_2O	2.307	0.3051	42	640 ± 10	95 ± 5	24	49
NiAl−	$Ni_{1.95}Al(OH)_{5.9}(CO_3)_{0.52}$, nH_2O	2.31	0.3030	63	420 ± 15	35 ± 7	49	47
CoAl−	$Co_{1.9}Al(OH)_{5.8}(CO_3)_{0.50}$, nH_2O	2.27	0.3062	57	430 ± 25	42 ± 10	47	45
ZnCr−	$Zn_{2.0}Cr(OH)_6(CO_3)_{0.42}Cl_{0.32}$, nH_2O	nd	nd	72	620 ± 25	31 ± 5	22	44
MgNiAl−	$Mg_{0.9}Ni_{1.1}Al(OH)_{6.4}(CO_3)_{0.5}$, nH_2O	2.310	0.3064	nd	520 ± 40	52 ± 20	37	53
MgCoAl−	$Mg_{0.95}Co_{0.9}Al(OH)_{5.7}(CO_3)_{0.50}$, nH_2O	2.285	0.3038	nd	550 ± 15	46 ± 7	33	52
MgAlFe−	$Mg_{1.85}Al_{0.5}Fe_{0.43}(OH)_{5.7}(CO_3)_{0.51}$, nH_2O	2.330	0.3083	nd	535 ± 10	41 ± 7	35	45

[a] Calculated from chemical analysis. [b] Assuming 3R stacking; nd, not detectable. [c] Estimated from SEM images. [d] Percentage calculated from TGA.

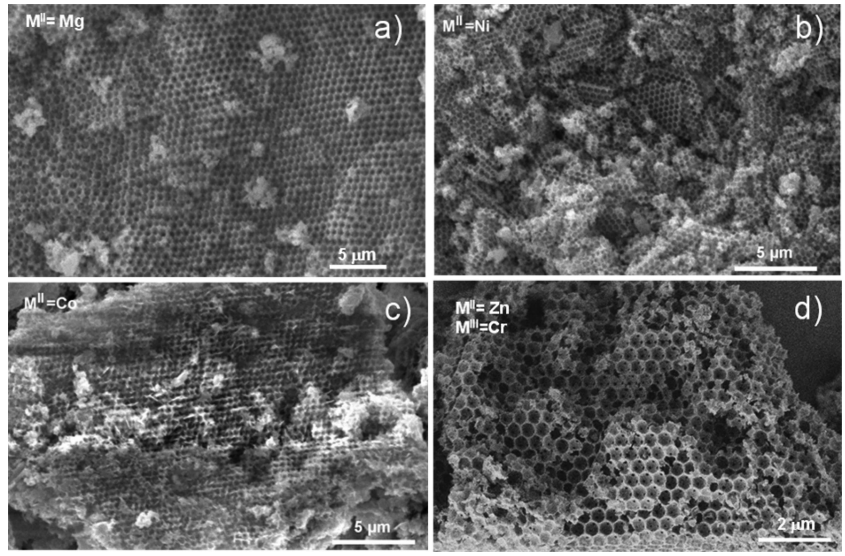

Figure 3. SEM images of ordered macroporous LDH with various compositions: (a) MgAl−, (b) NiAl−, (c) CoAl−, and (d) ZnCr−.

conducted in the absence of atmosphere control, the strong affinity of the LDH matrixes for carbonate anions induced a systematical contamination. For the ZnCr− matrix, the 00l lines of low intensity are very broad; this can be interpreted as a turbostratic disorder in the stacking long-range ordering and/or the presence of a side phase intercalated by a larger anion. This latter hypothesis is somewhat confirmed by the chemical analyses of the as-synthesized material (Table 1) which possesses chloride conjointly with carbonate, probably owing to the less basic character of this matrix. Furthermore, the low pH value (5.0) used during the template ZnCr− coprecipitation[13] does not favor the atmospheric CO_2 solubility in water. In parallel, chemical analyses indicate the absence of chloride for the other compositions, and the full charge compensation is occurring with the carbonate anions. On another hand, the experimental M^{II}/M^{III} ratios are near to those expected, that is, near to the starting salt solutions. SEM images of the as-obtained LDH are shown in Figure 3. In bulk aqueous solution, the LDH synthesis by coprecipitation traditionally leads to hexagonal platelets forming aggregates of micrometer size.[3] In these template conditions, all the LDH samples composed of MgAl−, NiAl−, CoAl−, and ZnCr− exhibit 3-DOM morphologies. It appears that during the LDH precipitation and crystal growth the PS array is maintained. The PS template dissolution appears to be an efficient way to liberate the porosity, leading to well ordered empty spheres. The removal of most of the polymeric component is confirmed elsewhere by IR spectra (see Supporting Information Figure S1). The spectra mainly exhibit the LDH characteristic bands, even if PS bands of small intensity are still present corresponding to residual PS absorbed on the surface of the inorganic materials. Because the starting PS array was imperfectly ordered, the resulting macroporous LDH replica clearly display different ordered domains (Figure 3). Pore sizes estimated from the SEM images range from 640 to 420 nm, which corresponds to a shrinkage of 22–49% in regard to the size of the starting PS beads (Table 1). Similar values were reported by other groups. However, such large variation in shrinkage is still not well understood.[43,53] The wall thickness in these samples ranges from 31 to 95 nm, resulting in nanoscale stacked platelets. In such a morphology, the inorganic component forms an interconnected wall-type structure, as illustrated in Figure 4a, on which the windows interconnecting the pores are well observed. These windows correspond to the contact points between the pristine PS beads. These channels are not, however, systematically observed because of the different levels of filling within the crystal during the impregnation steps. Tilting TEM images further evidence the 3-DOM structure as illustrated for the NiAl− composition in Figure 4. The different views of the pore array are consistent with views along the [111], [011], and [211] directions for replicas resulting from the fcc array.[55,69]

To investigate the inside porosity of the 3-DOM LDH, nitrogen adsorption experiments were performed (Table 1). The measured isotherms correspond to a type II H3 according

(69) Blanford, C. F.; Carter, C. B.; Stein, A. *J. Microsc. (Oxford)* **2004**, *216*, 263.

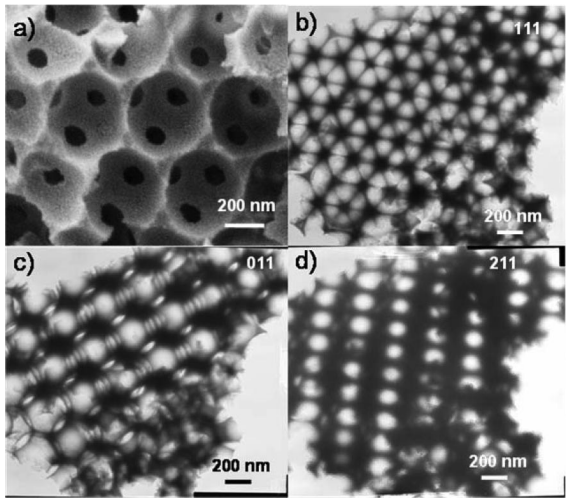

Figure 4. (a) SEM images of windows between macropores of NiAl− matrix and three tilting TEM images showing the (b) [111], (c) [110], and (d) [211] directions (fcc lattice) of the macroporous NiAl− matrix.

to the IUPAC classification,[70] characteristic of mesoporosity. However, the absence of a saturation plateau at high relative pressure indicates that the measured mesoporosity is mainly attributable to a nonrigid mesoporosity arising from interplatelet porosity as commonly observed for classic carbonate LDH phases.

From the catalytic application point of view, introducing more than two metal cations into the sheet is of great interest to access homogeneous mixed oxides.[7] The applicability of the colloidal crystal template method has thus been extended to more complex LDH compositions: MgAlNi−, MgCoAl−, and MgAlFe−. The XRD patterns associated with chemical analysis clearly evidence the homogeneous coprecipitation of the expected LDH phases (Figure 5). As previously noted, the variation of the *a* parameter is relevant to the modification of the composition. The 3-DOM structures are observed (Figure 5), although lower periodicity is obtained in the case of the MgAlNi− composition.

From the results above, it appears that the LDH phases prepared by the PS bead sacrificial template present X-ray characteristics of classical LDH-type materials; however, the associated diffraction lines are much broader (Figures 2 and 5), indicating a smaller coherence length. Indeed, TEM images have revealed that even if the LDH platelets were well ensconced in the voids, their shape was somehow ill-defined, and the layers were corrugated. To further investigate the macroporous solids and unravel whether the sequestration into the voids as well as the important apparent surface to bulk ratio affects the local structure, XAS was performed.

At first, conventional LDH phases prepared by the so-called coprecipitation method were used as the standard (see Supporting Information Figures S2 and S3). The modulus of the Fourier transform of the as-prepared LDH phases is then compared to the one obtained from the classical LDH-type parent materials (Figure 6). We observed that the polynomial extracted EXAFS oscillations of the macroporous LDH materials present similar features to those of the parent materials, and consequently, the moduli of the Fourier transforms are mostly superimposable. This has to be understood as a local structure around the central atom (Co, No, and Zn), quite similar among the corresponding phases, and as an absence of another byproduct, even an amorphous one, such as a single cation hydroxide that may be formed during the impregnation−precipitation procedure. However, the local environment was perused as the refinement was conducted in such a way that the number of surrounding atoms as well as their distance were free to move. The fit results deviate slightly (within the accuracy) from a starting hypothesis of six oxygen atoms composing P1 and six cations for P2. The quality of the fit is given in Figure 7. In more detail, the partition for P2 between divalent and trivalent cations is also close to 3:3 (Table 2). This ratio is expected from an ideal atomic arrangement present in LDH with a divalent to trivalent composition of 2.[71–73] Thus, we can infer from the refinements that the coprecipitation within the voids happens stochiometrically and according to the initial metal salt ratio. Two other humps visible on the modulus of the Fourier transforms are also superimposed to the corresponding contributions observed for the parent LDH-type materials (Figure 6). They are characteristic of backscattering atoms at a distance from the central atom of $a(3)^{1/2}$ and $2a$, respectively, a being the cell parameter. The latter, noted as P4, is largely enhanced by the so-called focusing effect as a result of the particular situation of three atoms lying linearly from each other and therefore increasing the π-backscattering effect.[74] The observation of such a contribution for the macroporous LDH materials and to an extent similar to the parent phases implies a similar degree of flatness of the inorganic sheets; therefore, one can conclude that the sequestration into the voids and the subsequent removal of the PS beads do not affect the local flatness of the LDH layers.

Thermal Behavior of 3-DOM LDH. The thermal behavior of the 3-DOM LDH phases was studied by *in-situ* XRD (Figure 8A). The data display a typical LDH decomposition scheme, according to the literature.[3] Upon moderate thermal treatment (250–400 °C), LDH matrixes are converted to mostly amorphous mixed oxides. When the calcination temperature is further increased above 800 °C, the respective line intensities of the oxides $M^{II}O$ and the spinel-like phases $M^{II}M^{III}{}_2O_4$ increase until 1000 °C. More specifically, for 3-DOM MgAl− and between 100 and 300 °C, a shift of the (00l) lines to smaller angles is observed on the diffraction patterns. This phenomenon has been extensively described[3,75] for the MgAl−carbonate phase and attributed to the bonding of carbonate anions with the layer (see Supporting Information Figure S5). The method of decomposition and the thermal products of LDH are not modified by the nanostructuration of the LDH particles. Identical thermal behavior is also evidenced by the TGA experiments on

(70) Rouquerol, F.; Rouquerol, J.; Sing, K. *Adsorption by powders and porous solids. Principles, Methodology and applications*; Academic Press: London, 1999.
(71) Belloto, M.; Rebours, B.; Clause, O.; Lynch, J.; Bazin, D.; Elkaim, E. *J. Phys. Chem.* **1996**, *100*, 8527.
(72) Hofmeister, W.; Platen, V. P. *Crystallogr. Rev.* **1992**, *3*, 3.
(73) Vucelic, M.; Jones, W.; Moggridge, G. D. *Clays Clay Miner.* **1997**, *45*, 803.
(74) Alberding, N.; Crozier, E. D. *Phys. Rev. B.* **1983**, *27*, 3374.
(75) Perez-Ramirez, J.; Abello, S.; van der Pers, N. M. *Chem. Eur. J.* **2007**, *13*, 870.

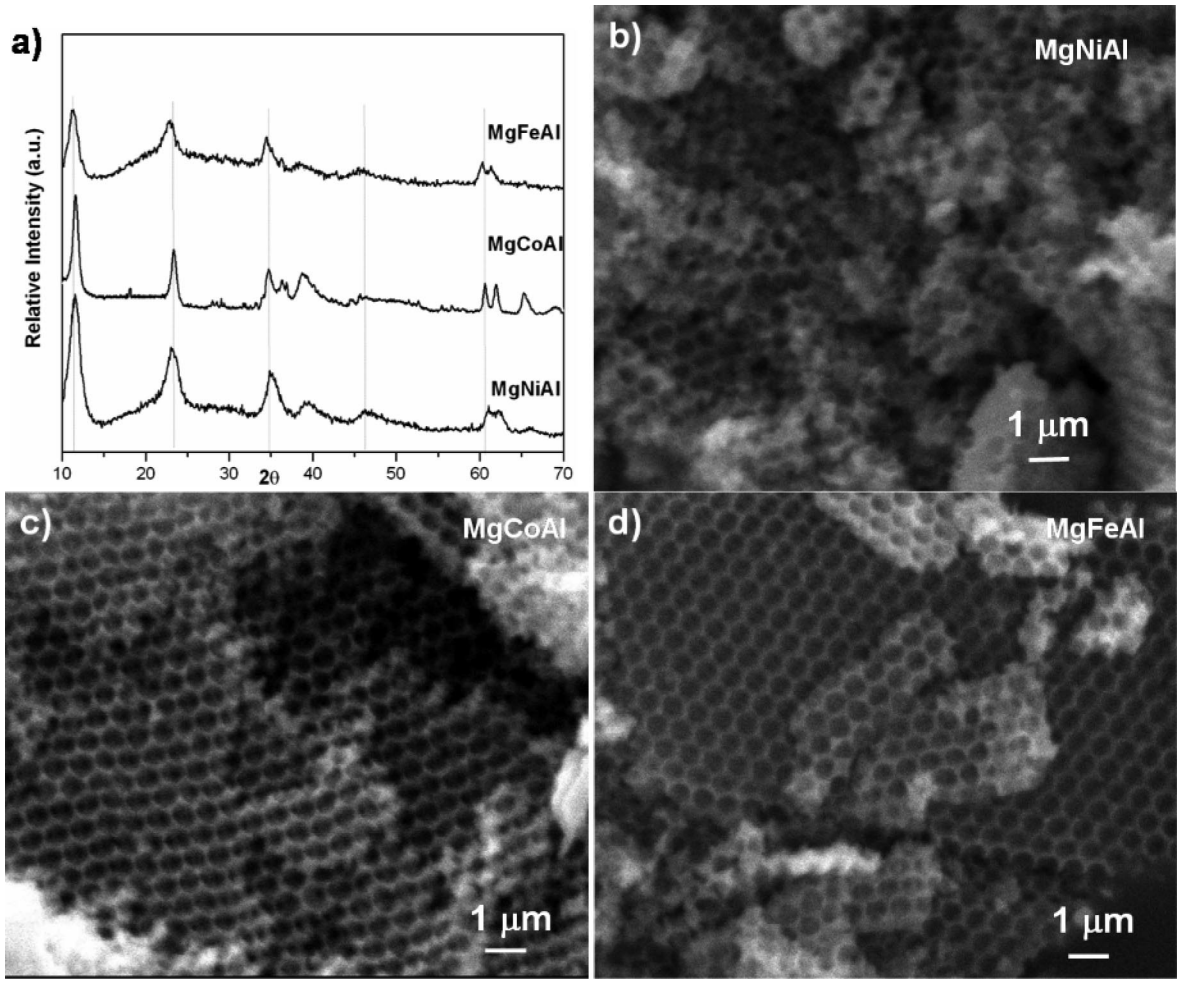

Figure 5. Powder XRD patterns and corresponding SEM micrograph of macroporous MgMAl−CO_3.

3-DOM LDH (see Supporting Information Figure S6) which display the expected steps of the decomposition. First, the dehydration occurs under 220 °C, followed by the dehydroxylation and the loss of the intercalated anion (carbonate) before 600 °C. These last two phenomena are concomitant, and the temperature of each step is related to the metal cations implied in the sheet. As already seen for coprecipitated phases, 3-DOM NiAl− and MgAl− appear more thermally stable than the 3-DOM ZnCr− and CoAl− matrixes, their dehydroxylation−decarboxylation steps being, respectively, centered at 360–370 °C and 300–320 °C. At 1000 °C, the total weight loss varied from 44% to 53% according to the matrix composition. Note that as illustrated in Figure 8B for the 3-DOM NiAl− matrix, an additional exothermic event is observed around 400 °C concomitantly with the endothermic dehydroxylation and decarbonation which corresponds to the combustion of residual adsorbed PS, already evidenced by IR spectroscopy (see Supporting Information Figure S1). The PS combustion is delayed in the case of the 3-DOM MgAl− at higher temperature (between 400 and 500 °C) probably because of the stronger interaction between the organic and inorganic components.

SEM images of the 3-DOM MgAl− and NiAl− calcined at both 400 and 800 °C (Figure 9a−d) clearly show that the macroporous structure is observed up to 800 °C. Nevertheless, the MgAl− behavior must be distinguished from the others. Indeed at 800 °C, no modification of the wall structure is observed for the MgAl− matrix, whereas for the other compositions and, in particular, for thermally treated NiAl− (Figure 9c−f), the thickness of the wall is obviously higher and spherical particles are present at the surface of the walls. In the latter case, TEM-EDX measurements evidenced NiO particles of about 100 nm in size, the walls being formed by an ill-crystallized spinel-like phase. The peculiar morphology observed for the calcined 3-DOM MgAl− should be correlated to the delay in oxide crystallization as evidenced by XRD measurements (Figure 8A). It should be emphasized that, upon thermal treatment from room temperature to 800 °C, the 3-DOM overall structure undergoes further shrinkage (28% for 3-DOM MgAl−) because the LDH thermal decomposition leads to smaller pores.

Interestingly, a macroporosity with about 500 nm diameter size is obtained for the phase 3-DOM MgAl− calcined at 400 °C, concomitantly with a surface area of 202 m^2/g (measured by the Brunauer−Emmett−Teller (BET) method). It shows the possibility of obtaining dual porosity for calcined mixed oxides phases, meso, and macroporosity.

Photocatalytic Activity of Intercalated Decatungstate. The photocatalytic activities of the decatungstate anions $W_{10}O_{32}^{4-}$ immobilized on both as-prepared 3-DOM MgAl− and standard coprecipitated MgAl− ($MgAl-_{stand}$) were

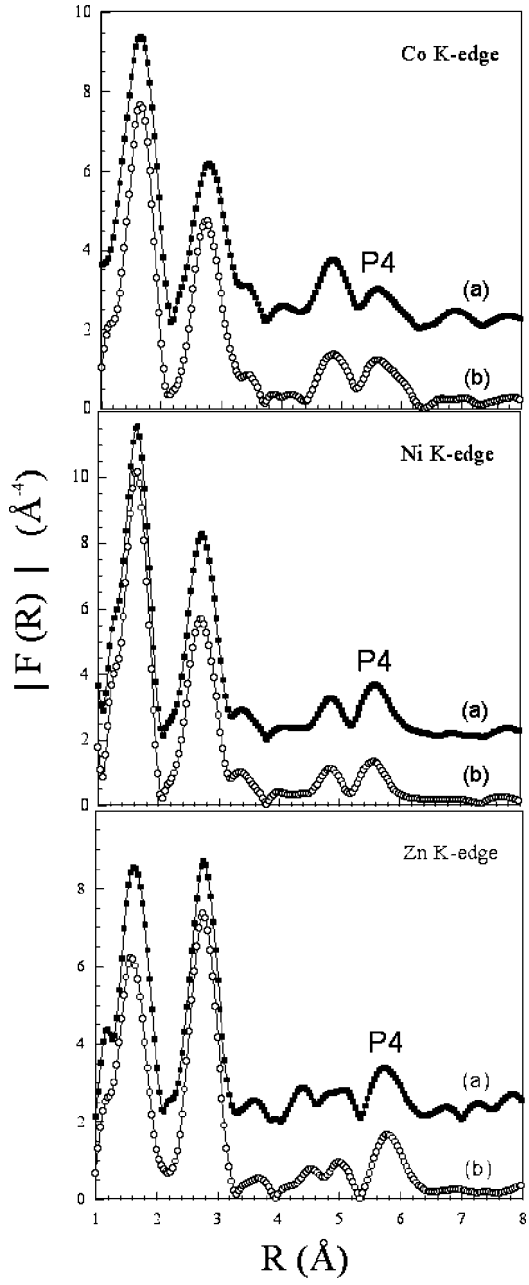

Figure 6. Comparison between the modulus of the Fourier transform spectra for Co_2Al-Cl (Co K edge), Ni_2Al-Cl (Ni K edge), and Zn_2Cr-Cl (Zn K edge) prepared by (a) classical coprecipitation and (b) sacrificial templating route. The distances are not corrected from phase shifts.

evaluated. The decatungstate anions display interesting photocatalytic activities which are of great interest in the degradation of organic pollutants and,[76,77] in particular, chlorophenols.[78] Satari and Hill[79] clearly showed that in the presence of oxygen $W_{10}O_{32}^{4-}$ allows the oxidation of the organic compounds and the effective cleavage of the carbon−halogen bonds. Irradiation of the decatungstate anions with solar light produces the excited state which is further able to oxidize organic products according Scheme 1.[80]

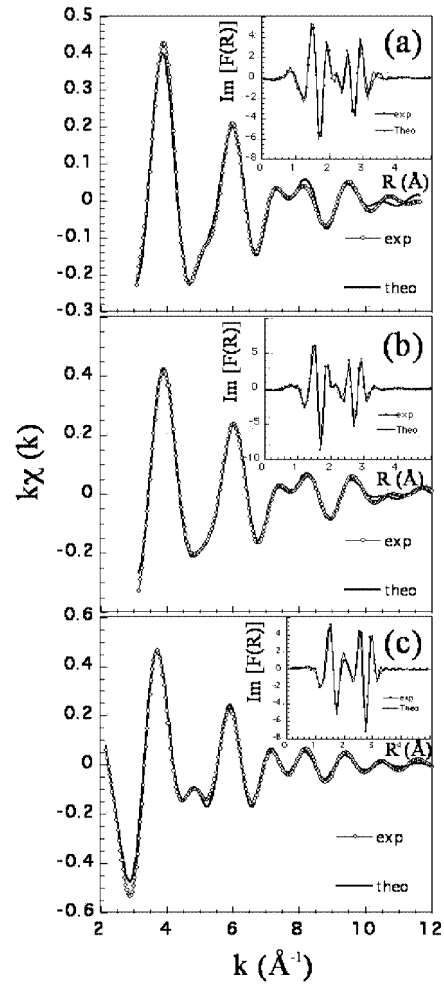

Figure 7. Refinement of the first two shells for the LDH phases prepared by the sacrificial templating route (a) Co_2Al-Cl (Co K edge), (b) Ni_2Al-Cl (Ni K edge), and (c) Zn_2Cr-Cl (Zn K edge). The corresponding imaginary part is displayed in the inset.

Table 2. Results of the EXAFS Refinements[a,b]

	bond	*N*	*R* (Å)	$\sigma^2 \times 10^{-3}$ (Å^2)	ρ (%)
Co_2Al	Co−O	6.0	2.07	7.5	
	Co−Co	2.8	3.13	10.6	
	Co−Al	3.4	3.08	13.9	1.3
Ni_2Al	Ni−O	6.1	2.05	6.2	
	Ni−Ni	3.4	3.11	10.4	
	Ni−Al	3.1	3.01	22.5	0.7
Zn_2Cr	Zn−O	6.1	2.07	6.6	
	Zn−Zn	3.2	3.15	8.3	
	Zn−Cr	2.6	3.11	14.2	1.1

[a] EXAFS parameters refined from LDH local structure (first two shells) were validated on LDH reference $Zn_2Cr-CO_3^{2-}$, Co_2Al-Cl, and Ni_2Al-Cl (see Supporting Information). [b] *N*, the coordination number; *R*, the distance; σ, the Debye–Waller factor; and ρ, the quality of the fit (see Experimental Section).

Because of the high solubility of $W_{10}O_{32}^{4-}$ and the difficulty to recover it from aqueous solutions, there is a great need to immobilize the decatungstate anions for environmental and technological applications.

Intercalation of the decatungstate anions was performed on LDH organically modified with an amphihilic anion, DDS, using the so-called guest displacement reaction.[2,3] DDS intercalated 3-DOM MgAl− was prepared through a calcination reconstruction process, as previously reported.[37,62] The enlarged basal spacing of the 3-DOM MgAl−DDS (2.57 nm)

(76) Hill, C. L. *Chem. Rev.* **1998**, *98*, 1.
(77) Maldotti, A.; Molinari, A.; Amadelli, R. *Chem. Rev.* **2002**, *102*, 3811.
(78) Mylonas, A.; Papaconstantinou, E. *J. Photochem. Photobiol., A* **1996**, *94*, 77.
(79) Sattari, D.; Hill, C. L. *Chem. Commun.* **1993**, 643.
(80) Tanielian, C. *Coord. Chem. Rev.* **1998**, *178–180*, 1165.

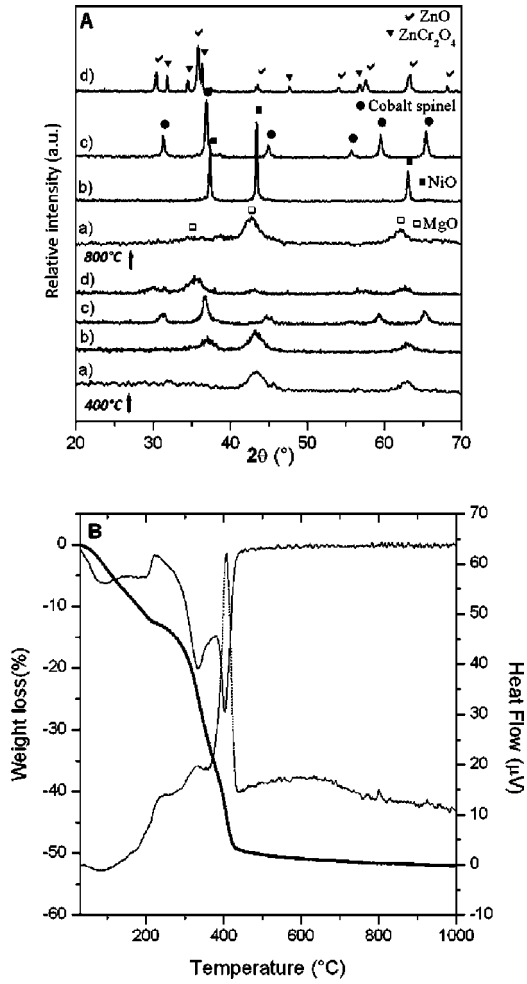

Figure 8. (A) Powder XRD patterns for (a) MgAl−, (b) NiAl−, (c) CoAl−, and (d) ZnCr− heated at 400 and 800 °C and (B) TGA, DTG, and DTA of 3-DOM NiAl−.

favors the exchange of the cumbersome and reactive decatungstate anion. After completion of the reaction, the (00l) diffraction lines shift to high theta values because of the contraction of the interlayer galleries ($d = 1.1$ nm). The XRD patterns are characteristic of POM containing LDH, although presenting a low crystallinity as already emphasized for POM intercalated into classically prepared LDH (see Supporting Information Figure S7).[81,82] FTIR spectra (Figure 10a) clearly evidence the loss of the vibration bands characteristic of the DDS anion after the exchange reaction, replaced by the ν_{W-O} and ν_{O-W-O} stretching and bending modes of the decatunsgtate species, slightly shifted about 20–30 cm^{-1} to lower energy. The LDH structure undergoes a topotactic exchange process while maintaining the lattice vibrations in the low energy region ($\nu_{Mg,Al-O}$ and $\nu_{O-Mg,Al-O}$ at 659 and 445 cm^{-1}, respectively). The decatungstate intercalated in the coprecipitated MgAl−LDH displays the same structural properties (XRD, FTIR not shown here). It is, however, noteworthy that the macroporosity is maintained for the 3-DOM MgAl−$W_{10}O_{32}$ through the anion exchange process (Figure 10b).

(81) Rives, V.; Ulibarri, M. A. *Coord. Chem. Rev.* **1999**, *181*, 61.
(82) Sels, B. F.; De Vos, D. E.; Jacobs, P. A. *Stud. Surf. Sci. Catal.* **2000**, *129*, 845.

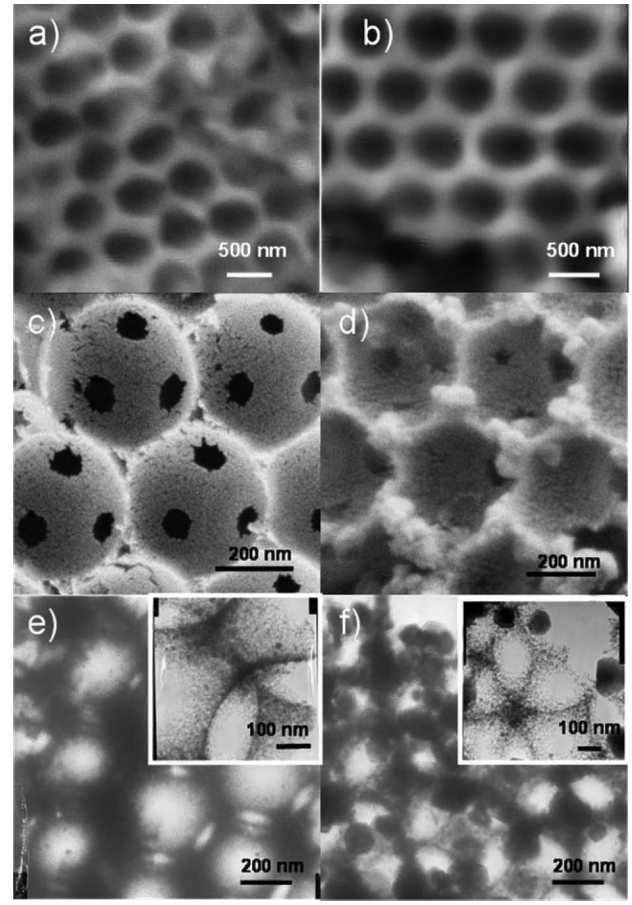

Figure 9. SEM images of MgAl− heated at (a) 400 °C and (b) at 800 °C and NiAl− heated at (c) 400 °C and (d) 800 °C and corresponding TEM images of NiAl− heated at (e) 400 °C and (f) 800 °C.

Scheme 1. Schematic Photocatalytic Activity of Decatungstate from Reference 80

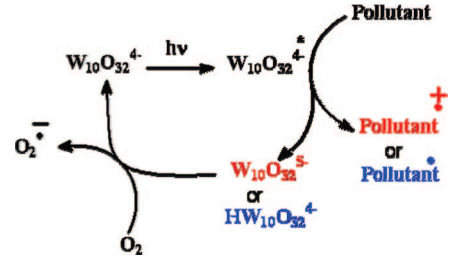

The evaluation of photodegradative properties of both decatungstate intercalated LDH 3-DOM MgAl−$W_{10}O_{32}$ and MgAl−$W_{10}O_{32stand}$ was performed. The irradiation of the photocatalyst/DMP mixture (1.0 g L^{-1}/1.0 mol L^{-1}) was performed in an air saturated solution at 365 nm. Under these conditions, the incident light was specifically absorbed by the photocatalyst.

Figure 11 reports the evolution of the DMP concentration. As clearly shown, the degradation of the organic pollutant was not effective for MgAl−DDS and at less than 10% for MgAl−$W_{10}O_{32stand}$. In contrast, a rather efficient degradation was observed with the 3-DOM MgAl−$W_{10}O_{32}$ in the early irradiation times without any sign of a lag period, and a total disappearance was observed within 70 h of irradiation time. It is worth noting that, under our similar experimental

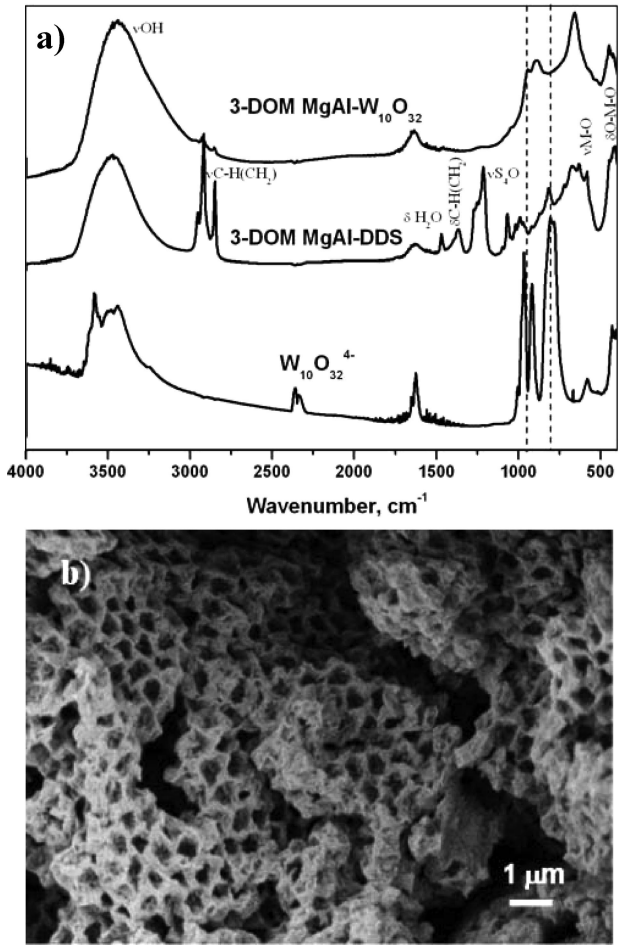

Figure 10. (a) FTIR spectra of $W_{10}O_{32}^{4-}$, 3-DOM MgAl−DDS, and 3-DOM MgAl−$W_{10}O_{32}$. (b) SEM images of 3-DOM MgAl−$W_{10}O_{32}$.

conditions, no disappearance was observed when the photocatalyst was removed from the solution. These results highlight the role played by the immobilized $W_{10}O_{32}^{4-}$ in such an open macroporous framework. As evidenced by the HPLC experiments, the degradation of DMP yields to the formation of two main byproducts with short retention times: 2,6-dimethylhydroquinone and 2,6-dimethylbenzoquinone.[83,84] They were identified by comparison with the standard features. They were formed through a one electron oxidation initiated by the excitation of $W_{10}O_{32}^{4-}$.

These results clearly demonstrate the enhanced photocatalytic properties of the decatungstate intercalated into a macroporous LDH structure. Obviously, macroporous LDH materials drastically increase the accessibility of light to the intercalated decatungstate and the DMP diffusion, evidencing that nanostructuration of the LDH plays a key role in the

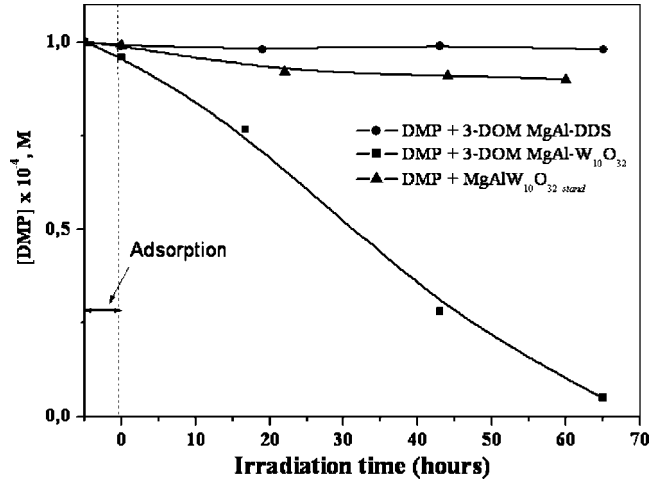

Figure 11. Kinetic data of DMP photodegradation by 3-DOM MgAl−DDS, MgAl−$W_{10}O_{32stand}$, and 3-DOM MgAl−$W_{10}O_{32}$.

photocatalytic performance. Such behavior associated with our recent results on the superior adsorption properties of 3-DOM hydrotalcite[85] underlines the interest for the development of LDH materials with wide-open frameworks.

Conclusion

By using a template colloidal crystal coprecipitation, various 3-DOM LDH have been prepared showing the applicability of such a templating route for LDH phases. Room temperature 3-DOM LDH phases present features similar to those of the chemically made parent phases, in terms of mesoporosity and thermal behavior, but with no possible distinction at the local scale. Arrestingly, calcined 3-DOM LDH phases sustain a macroporous ordering even at high temperatures, making them promising for framework building precursors. Finally, results obtained on DMP photodegradation by decatungstate intercalated LDH evidenced the enhanced properties of the macroporous LDH materials, showing that the 3-DOM LDH might improve the LDH performance in various potential applications.

Acknowledgment. The authors thank Valerie Briois, François Villain, and Luca Olivi for their help during the EXAFS measurements, the European Community for the transnational access to the Elettra Synchrotron Facility, and the CNRS for supporting the LURE-Elettra mutual agreement. Thanks to A.M. Gélinaud from Casimir for microscopy facilities.

Supporting Information Available: Additional figures are provided (PDF). This material is available free of charge via the Internet at http://pubs.acs.org.

CM702755H

(83) Mazellier, P.; Bolte, M. *Chemosphere* **1997**, *35*, 2181.
(84) Mazellier, P.; Sarakha, M.; Rossi, A.; Bolte, M. *J. Photochem. Photobiol., A* **1998**, *115*, 117.
(85) Geraud, E.; Bouhent, M.; Derriche, Z.; Leroux, F.; Prevot, V.; Forano, C. *J. Phys. Chem. Solids* **2007**, *68*, 818.